A Fast and Accurate Global Maximum Power Point Tracking Method for Solar Strings Under Partial Shading Conditions

S.M. Hashemzadeh, M. Hejri[*]

Department of Electrical Engineering, Sahand University of Technology, Tabriz, Iran.

Abstract- *This paper presents a model-based approach for the global maximum power point (GMPP) tracking of solar strings under partial shading conditions. In the proposed method, the GMPP voltage is estimated without any need to solve numerically the implicit and nonlinear equations of the photovoltaic (PV) string model. In contrast to the existing methods in which first the locations of all the local peaks on the P-V curve are estimated and next the place of the GMPP is selected among them, the suggested method estimates directly the GMPP without any need for the evaluation of the other local peaks. The obtained GMPP voltage is then given as a reference value to the input voltage controller of a DC-DC boost converter to regulate the output voltage of the solar string at the GMPP voltage in various irradiation conditions. Furthermore, the values of the temperature and irradiation level of each PV module within the PV string are estimated, and therefore, the proposed method does not need to thermometers and pyranometers. This makes it as a reliable and low-cost GMPP tracking method. The theoretical aspects on which the proposed GMPP algorithm is established are also discussed. The comparison of the numerical results of the suggested GMPP tracking scheme with the existing methods at different environmental conditions shows the satisfactory operation of the proposed technique from the speed and accuracy point of views.*

Keyword: Global maximum power point; Model-based GMPP techniques (GMPP); Partial shading; PV strings.

1. INTRODUCTION

In recent years, due to the high costs of fossil resources, their gradual decrease and environmental pollution issues, the use of renewable-energy resources is expanding day-to-day. In this regard, the solar energy has attracted much attention in industry and academia because of its significant benefits such as low maintenance and operational costs and more compatibility with the environment [1, 2]. It has been estimated that the solar energy received by the earth is ten thousand times more than the world's energy consumption needs, and therefore, it can be considered as an endless energy resource [3]. Hence, the use of photovoltaic (PV) technology to generate electrical energy is growing day-to-day in a wide range of power ratings and in a variety of applications [4].

Since PV systems still offer low efficiency and high initial costs, some methods are required to extract the maximum power from PV systems [5, 6]. On the other

hand, the power-voltage (P-V) characteristic of solar arrays is nonlinear and contains only one peak point under uniform radiation conditions whose location depends on the temperature and irradiation level of the PV array [7, 8].

Due to the nonlinear and time-varying nature of the maximum power point position, several methods have been introduced in the literature for the maximum power point tracking (MPPT) under uniform irradiation conditions [9, 10]. However, in real-world applications, especially in urban areas, non-uniform irradiation conditions are created due to the space limitations and existing obstacles in the installation places of PV arrays [11]. The non-uniform irradiation condition, called as partial shading condition, causes that the current-voltage (I-V) characteristic of the solar arrays to be more complex and several local peaks to appear on the P-V curve [12, 13]. At these conditions, using conventional MPPT methods can cause significant losses in extracting the maximum power from the PV array [14]. Hence, the convergence to the global maximum power point in partial shading conditions has become a challenging issue.

There are several methods to track the GMPP in partial shading conditions of which one can mention to reconfiguration of PV arrays [15-17], meta-heuristic

algorithms [1, 5, 18-20] and model-based approaches [21-26]. The reconfiguration methods rely on the reconfiguration of PV arrays and offer high costs due to the use of many diodes and switches in the PV arrays structure. Meta-heuristic based approaches are accurate in finding the GMPP under partial shading conditions; however, due to their repetitive nature, they offer low convergence rate, and as a result, high tracking time. The main advantage of the model-based MPPT techniques is their high speed to find the GMPP. Compared to the meta-heuristic based techniques, a limitation of model-based MPPT methods is to use a number of sensors to calculate the GMPP. Hence, the model-based methods are more costly than the heuristic-based algorithms. Nevertheless, the precision and especially the GMPP tracking speed in model-based methods is very high in a wide range of climatic conditions, which increases the efficiency of the overall system. These advantages compensate some parts of the costs in the model-based tracking techniques. Furthermore, the information provided by the voltage and current sensors can be used to identify the type and location of any fault in the photovoltaic array. These advantages associated with the model-based GMPPT methods are the main motivations for this research.

In Ref. [25], a model-based approach has been proposed to find the maximum power point only for a PV module and its applicability to detect the GMPP of PV arrays under partial shading conditions has not been discussed. In Ref. [26], an MPPT technique is proposed based on the combination of the model-based and perturb and observe (P&O) methods. The technique has been applied to only one PV module and its ability to track the GMPP for PV arrays under partial shading conditions has not been investigated. A model-based MPPT approach for PV arrays under partial shading conditions has been presented in Ref. [27] based on the Lambert equations of the PV modules. To find the GMPP, the partially shaded PV array has been modeled as a set of nonlinear equations solved using numerical techniques such as Newton-Raphson method. From the drawbacks of this method, one can mention its complexity and higher computational burden and the possibility of numerical divergence due to the poor choice of initial conditions. In Ref. [28], a model-based MPPT method has been proposed for PV arrays under partial shading conditions considering two limiting conditions: 1) the existence of only two different irradiation levels in the PV array, and 2) assuming a lower bound of 100 W/m^2 for the irradiation level. In Ref. [21], some relations have been presented to estimate all the local peaks on the P-V curve of a partially shaded PV string. In the proposed technique, the series and parallel resistances have been ignored in the model of PV modules and the effect of the temperature changes on the P-V curve peaks has not been considered. In Ref. [22], the current and voltage of local peaks on the P-V curve of a partially shaded PV string are estimated using some empirical relations. In these relations, the effect of temperature changes on the estimated coordinates of the local peaks has not been considered. Next, the values of the respective local power peaks are calculated by multiplying the voltage and current values of the individual local peaks. Finally, the location of the GMPP is detected by the comparison of the resulting local peak powers. The approach in Ref. [22] has been modified and extended to multi-string PV arrays in Ref. [23].

In this paper, the coordinate of the GMPP on the P-V curve is directly estimated without needing to solve numerically the nonlinear equations of the PV string I-V characteristic. Unlike the existing methods by which first the coordinates of all local optima points are estimated, and then the GMPP is chosen among the estimated local peaks, in the proposed technique, the GMPP is directly estimated without calculating the other local peaks, and therefore, results in less computational burden as compared with the existing methods. The calculated GMPP voltage is given as a reference value to the input voltage controller of a DC-DC boost converter connected between the PV string and load. Hence, the partially shaded PV input voltage is regulated at the GMPP voltage, and the global maximum power point is tracked. Furthermore, the temperature and irradiance level of each module is estimated using the PV module model, and therefore, there is no need for thermometers and pyranometers. The technical basis in this work is the approach proposed by the authors of the present paper in [24] for the PV arrays modified for a PV string with two major differences. In Ref. [24], when the approach is adapted for the PV arrays, we still need to use iterative numerical techniques to solve a set of nonlinear algebraic equations. Therefore, although apparently a more general problem has been solved in Ref. [24], but unfortunately it is less applicable due to the time-consuming iterative numerical solutions as well as the danger of the iterations' divergence because of possible unsuitable selection of initial conditions. On the other hand, in the present work for the PV strings, we do not need to use any numerical solutions of any nonlinear algebraic equation. Another point that distinguishes our

present work from Ref. [24] is a discussion on the theoretical aspects on which the proposed GMPP algorithm has been established. Using numerical simulations, the proposed technique is compared to the methods in references [21, 22, 25] from the degree of accuracy point of the view.

The remainder of the paper is organized as follows. Section 2 deals with the mathematical modelling of the PV modules. The effect of partial shading on the P-V and I-V curves of the PV strings is described in Section 3. In Section 4, the proposed GMPP tracking method is presented. Section 5 deals with the estimation procedure of the temperature and irradiation levels of the PV modules within PV strings. In Section 6, the simulation results are presented, and a comparative study is performed between the proposed GMPP tracking method, and the methods presented in references [21, 22, 25]. Finally, the concluding remarks are made in Section 7.

2. THE MATHEMATICAL MODEL OF PV MODULE

In this paper, the single-diode model of PV modules is used considering the series and parallel resistances as shown in Fig. 1.
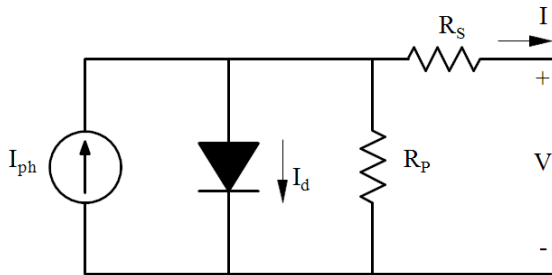

Fig. 1. The single-diode model of a PV module

The model parameters are determined based on the proposed technique in Ref. [29]. The current-voltage (I-V) relation is given by Eq. (1).

$$I = I_{ph} - I_0 \left[\exp\left(\frac{V + IR_s}{aV_t}\right) - 1 \right] - \frac{V + IR_s}{R_p} \qquad (1)$$

where I_{ph} is the PV module photocurrent generated from the solar radiation received by the PV module surface and is calculated by Eq. (2), I_0 is the diode reverse saturation current and given by Eq. (3), R_s and R_p are PV module series and parallel resistances respectively and a is the diode ideality factor. V_t is the PV module thermal voltage calculated by Eq. (4).

$$I_{ph} = \left(I_{ph,n} + k_i \left(T - T_i\right)\right) \frac{G}{G_n} \qquad (2)$$

$$I_0 = \frac{I_{ph} - \dfrac{V_{oc,n}}{R_p}}{\exp\left(\dfrac{V_{oc,n}}{aV_t}\right) - 1} \qquad (3)$$

$$V_t = \frac{N_s kT}{q} \qquad (4)$$

In Eq. (2) and Eq. (3), G is the irradiation level on the PV module surface, k_i is the temperature coefficient of the short-circuit current, $I_{ph,n}$ and $V_{oc,n}$ are the PV module photocurrent and open-circuit voltage under Standard Test Conditions (STC) $\left(\text{T}_n=25 \ \& \ \text{G}_n=1000 \ \frac{\text{W}}{\text{m}^2}\right)$. In. Eq. (4), N_s is the number of series connected PV cells within the PV module, q is the elementary charge $\left(1.60217646\times10^{-19}\,C\right)$, k is Boltzmann's constant $\left(1.3806503\times10^{-23}\,\frac{\text{J}}{\text{°K}}\right)$ and T is the PV module surface temperature.

3. THE EFFECT OF PARTIAL SHADING ON THE PV STRING I-V AND P-V CURVES

The PV *modules* are manufactured from the series connection of PV *cells* to achieve high power and voltage levels [28, 29]. PV modules are connected in series as a PV string to obtain a higher voltage level. To achieve high-power levels the PV strings are connected in parallel to form PV *arrays* [29]. In this paper, our focus is on the PV strings. Fig. 2(a) shows a PV string under uniform irradiation conditions in which all the series connected modules generate equal photocurrents. As can be seen in Fig. 2(b), if the irradiation levels of PV modules within the PV string are different, then the partial shading effect occurs. In these conditions, the shaded modules produce less photocurrent compared with the PV string output current. As a result, the difference between the shaded PV module photocurrent and the PV string current passes from the parallel resistance of the shaded PV module and a large negative voltage is created across shaded PV modules. If this negative voltage reaches the PV module breakdown voltage, then the hot-spot phenomenon occurs. The result is that the PV module is damaged and will not be able to generate power. To avoid this phenomenon, a reverse diode is connected across the PV module called as a bypass diode. The bypass diode creates a short circuit across the shaded PV module and prevents the hot-spot phenomenon. In this case, several steps are created on the I-V and P-V curves of the PV string. Fig. 3 shows the I-V and P-V curves of a PV string consisting of three series connected PV modules (see

Fig. 2) each of which is subject to a different irradiation level. According to this figure, one can see that corresponding to each level of irradiation, a power peak on the P-V curve and a step in the I-V curve is created.
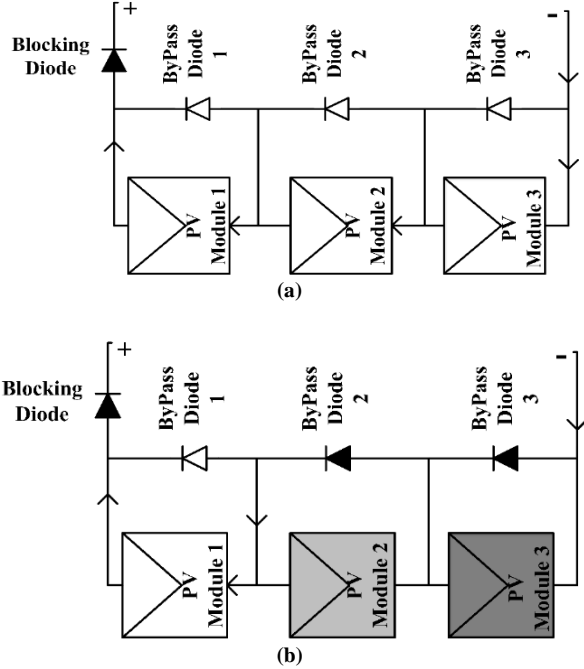

(a)

(b)

Fig. 2. A PV string consisting of series connected PV modules and bypass diodes. (a) PV string under STC, (b) PV string under partial shading
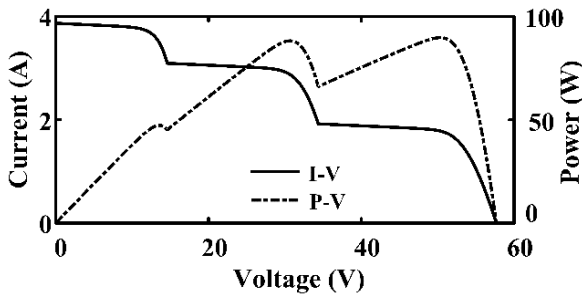

Fig. 3. P-V and I-V characteristics under partial shading

4. GLOBAL MAXIMUM POWER POINT TRACKING FOR A PV STRING UNDER PARTIAL SHADING CONDITIONS

In the proposed method, to track the GMPP, first the voltage and current of all PV modules within the PV string are measured via voltage and current sensors. Then, the maximum power point voltage of each module $V_{m,i}$ is calculated by Eq. (5) [30].

$$V_{m,i} = \frac{V_m(G_n)}{1 + \delta \ln\left(\dfrac{G_i}{G_n}\right)} + k_v(T_i - T_n) \tag{5}$$

In (5), k_v is the open-circuit voltage temperature coefficient, $V_m(G_n)$ is the PV module MPP voltage at STC, T_n is the PV module temperature at STC, T_i is the i-th PV module temperature, and δ is a dimensionless constant whose value is set to 0.05 for multi-crystalline PV modules [30]. In the sequel, to consider the effect of bypass diodes on the shaded PV modules, the conditions of Eq. (6) are applied.

$$\begin{cases} V_i = -V_d & :Bypass\ diode\ is\ ON \quad and \quad x_i=0 \\ V_i > 0 & :Bypass\ diode\ is\ OFF \quad and \quad x_i=1 \end{cases} \tag{6}$$

where V_i is the i'th PV module voltage within PV string whose value is measured using a voltage sensor and x_i is an integer whose value is set to zero whenever the PV module is short-circuited via the corresponding bypass diode. Otherwise, its value is set to 1. The voltage V_d is the forward voltage across the bypass diodes whose value is set to $0.8\,V$ in this paper. During the numerical simulations, it has been observed that at the GMPP the MPP voltage of PV modules under high radiation levels can be better estimated by Eq. (7) instead of Eq. (5). In the sequel, this issue is further investigated. The criterion for high irradiation level relies on the comparisons between the PV modules measured voltage, and its estimated maximum power point voltage calculated by Eq. (5). This means that to improve the quality of estimations, whenever the PV module measured voltage is greater than the value obtained from Eq. (5), then the PV module peak voltage is calculated by Eq. (7) instead of Eq. (5).

$$V_{m,i} = M \times V_{oc,n} \tag{7}$$

where M is a proportional constant. To estimate the value of M, 50 various radiation patterns are simulated. In each case, the value of M is calculated as the ratio of the fixed voltages of the PV modules with the maximum radiation at the GMPP to their open-circuit voltage value at STC.
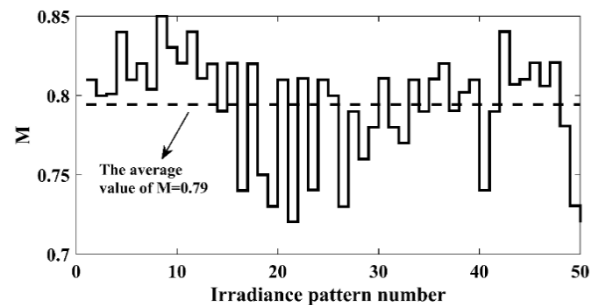

Fig. 4. The values of M (solid line) and its average (dashed line) over 50 different radiation patterns

As it can be seen from Fig. 4, the value of M is varying between 0.72 and 0.85 whose average value during 50 simulated irradiation patterns is 0.79. Hence, in this paper, the value of M is set to 0.79.

According to Eq. (6) and writing a Kirchhoff's Voltage Law (KVL) around the PV string of Fig. 8, one can reach.

$$V_{string} = \sum_{i=1}^{n_s} \left[x_i \times V_i - (1 - x_i \times V_d) \right] \qquad (8)$$

where V_{string} is the PV string voltage. Next, we use Eq. (8) to estimate the global maximum power point voltage of the PV string, i.e., $V_{m,string}$. Since it is targeted to obtain the maximum power from the PV string, it is expected that the required operating point of each PV module within PV string is around its maximum power point (MPP) whose voltage, $V_{m,i}$, can be estimated by Eq. (5) or Eq. (7). Therefore, by substituting $V_i = V_{m,i}$ into Eq. (8), one can estimate $V_{m,string}$ as

$$V_{m,string} = \sum_{i=1}^{n_s} \left[x_i \times V_{m,i} - (1 - x_i) \times V_d \right] \qquad (9)$$

Since Eq. (9) is an approximate formula, the equality sign " $=$ " in Eq. (9) must be interpreted as an approximate equality sign "$\approx$". To see what the values of the PV modules are at the global maximum power point, a PV string consisting of 10 modules is considered as shown in Fig. 5. This PV string is connected to a variable voltage source with a ramp waveform whose value changes from zero to the string nominal open-circuit voltage.

The simulation results are shown in Fig. 6. Fig. 6(a), Fig. 6(b) and Fig. 6(c) show the module voltages with irradiation levels of 1000 W/m^2, 500 W/m^2 and 100 W/m^2 respectively. In these figures, the circle sign stands for the actual value of the PV modules voltage at the GMPP, the multiplication sign shows the PV modules MPP voltage calculated by Eq. (5), and the star sign stands for the PV modules' voltage computed by Eq. (7). Fig. 6(d) illustrates how PV string power evolves over time.

4.1. The origin of the approximations in equation (9) to estimate the GMPP voltage

Here, the significant principles on which Eq. (9) has been developed, is discussed. Let us consider Figs. 2(b) and 3. Fig. 3 shows the I-V and P-V curves of a PV string consisting of three series connected PV modules each of which is subject to a different irradiation level (see Fig. 2(b)). According to these figures, one can realize that bypassing of diodes across PV modules depends on the PV string current. For example, as can be seen from Fig. 3, at current 1 A, none of PV modules is bypassed, at current 2.5 A only 1 module is bypassed, at 3.5 A there are 2 bypassed modules. According to these figures, one can see that the global peak power in the overall P-V curve is always aligned with one of the local peaks created on the P-V curve. Therefore, if one can calculate or estimate the coordinates of these local peaks, the coordinate of the global peak is obtained easily by comparison of all of these local peaks. In this regard, Eq. (9) is an approximate formula that gives the local peaks of the P-V curve in various situations of the bypass diodes. Let us consider the following various cases to justify how Eq. (9) gives a suitable estimation of the GMPP voltage candidates. In the following analysis, without loss of generality, it is assumed that $G_1 > G_2 > G_3$ where G_i, $i \in \{1,2,3\}$ is the radiation of the ith PV module within PV string of Fig. 2(b).

A: Two of PV modules are bypassed
In this case, only one of the modules (the module with the highest irradiation level of G_1) remains to supply power, and as a result, it is physically evident that the maximum power of this module is obtained in its maximum power point voltage $V_{m,1}$ estimated by Eq. (5) or Eq. (7). Since the other two modules are bypassed, the KVL across the PV string terminals implies that $V_{m,string} = V_{m,1} - 2V_d$. In fact, this voltage corresponds to the most left local peak voltage in Figure 3.

B: Only one of the PV modules is bypassed
In this case, the module with the lowest irradiation level (G_3) is bypassed and the next two modules with the medium and highest irradiation levels $(G1 \& G2)$ supply the power. At this situation, we should estimate the PV string voltage corresponding to the middle local peak of Figure 3. At this point, the PV string current is equal to the MPP current of the PV module with the medium radiation level, i.e., $I_{m,2}$.

As a result, the voltage of PV module with medium radiation level is its MPP voltage ($V_{m,2}$) and the voltage across the PV module with the highest radiation level is determined by its I-V curve at $I_{m,2}$. Here is the point that we approximate the PV module voltage with the highest irradiation level by its own MPP voltage, i.e., $V_{m,1}$. As a result, based on the KVL across the PV string terminals, (9) approximates the PV string voltage at the middle local peak by $V_{m,1} + V_{m,2} - V_d$.
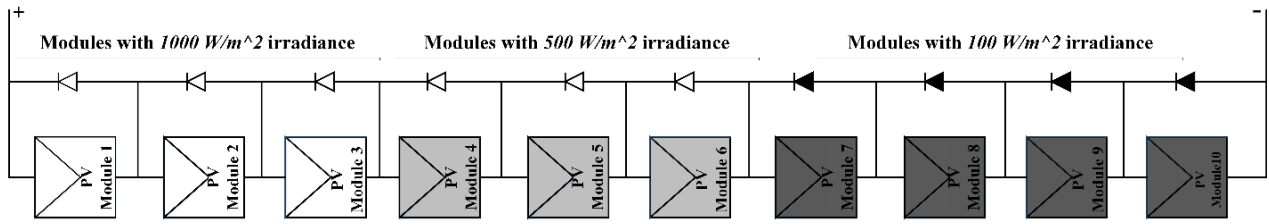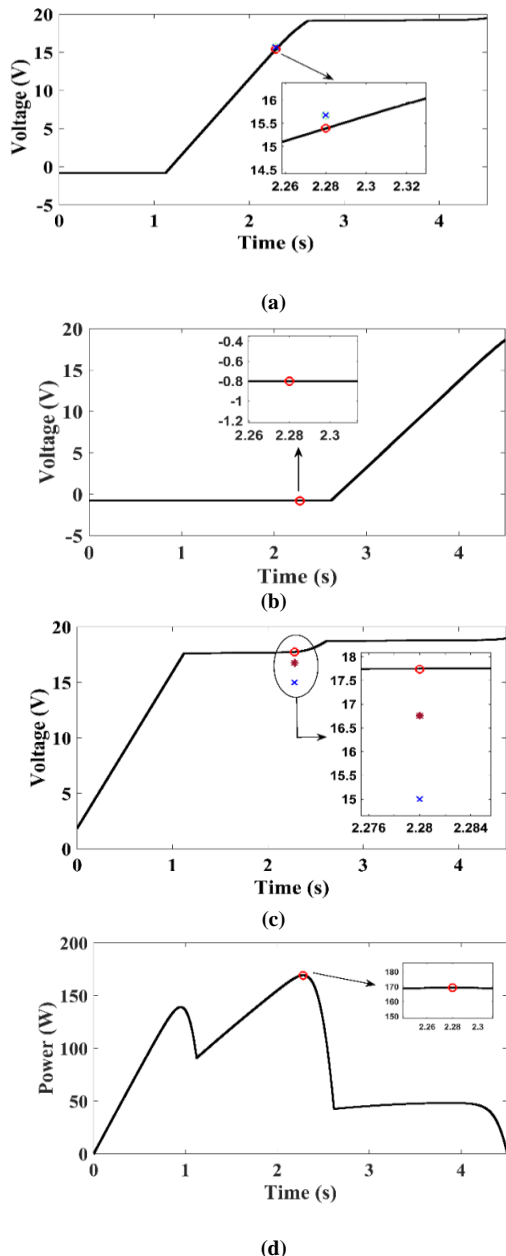
Fig. 5. A PV string consisting of 10 PV modules

(a)

(b)

(c)

(d)

Fig. 6. The voltage and power waveforms of the PV string of Figure 5. (a) PV modules voltage under irradiation level of 1000 $\left(\frac{W}{m^2}\right)$, (b) PV modules voltage under irradiation level of 500 $\left(\frac{W}{m^2}\right)$, (c) PV modules voltages under irradiation level of 100 $\left(\frac{W}{m^2}\right)$, (d) the PV string output power profile

C: None of PV modules are bypassed

In this case, the PV string current is determined by the MPP current of the PV module with the lowest irradiation level, i.e., $I_{m,3}$. Therefore, the voltage across the PV module 3, is $V_{m,3}$. The voltage across the PV modules 1 and 2 are determined by their I-V curves evaluated at the current $I_{m,3}$. Again in our technique, these voltages are approximated by the MPP voltage of these modules, i.e., $V_{m,1}$ and $V_{m,2}$. As a result, the KVL across the PV string terminals implies that the most right local peak voltage of Figure 3 is approximated to $V_{m,1}+V_{m,2}+V_{m,3}$ as given by Eq. (9). The foregoing analysis can be extended to a PV string with n_s series connected PV modules and therefore the general formula (9) is verified.

4.2. The proposed GMPPT algorithm

The flowchart of Fig. 7 illustrates the step-by-step stages of the proposed global maximum power point tracking method for PV strings consisting of n_s series connected PV modules with their anti-parallel bypass diodes. According to the proposed algorithm in Figs. 7, Eqs. (6) and (9) are iteratively calculated until a convergence is achieved around the GMPP. During each iteration the turning on and off of the bypass diodes are checked, and PV modules' voltages are measured via the voltage sensors across the PV modules within the PV string.

This gives the values of binary constants x_i of Eq. (6). Next, using these binary values, the GMPP voltage of the PV string is estimated via Eq. (9) in which the value of the parameter $V_{m,i}$ is evaluated using Eq. (5) or Eq. (7). The GMPP voltage is fed to the DC-DC converter to regulate the output voltage of the PV string at the calculated reference voltage via Eq. (9). During this voltage regulation, the situation of the bypass diodes may change, and as a result, the new reference voltage must be calculated via Eqs. (6) and (9). This process is iterated several times until the situations of the bypass diodes are kept constant, and a convergence is obtained. As far as the radiation pattern and intensity are constant over the PV modules of the PV string, the bypass diodes turning on and off situations are constant and the GMPP

coordinate is not changed. As soon as the radiation pattern is changed, the new value of the PV string GMPP voltage is evaluated through the same preceding proposed algorithm. The validity of the equations in Eq. (6) and Eq. (9) employed within the algorithm of Fig. 7, is shown via extensive simulation results and comparative studies presented in Section 6.
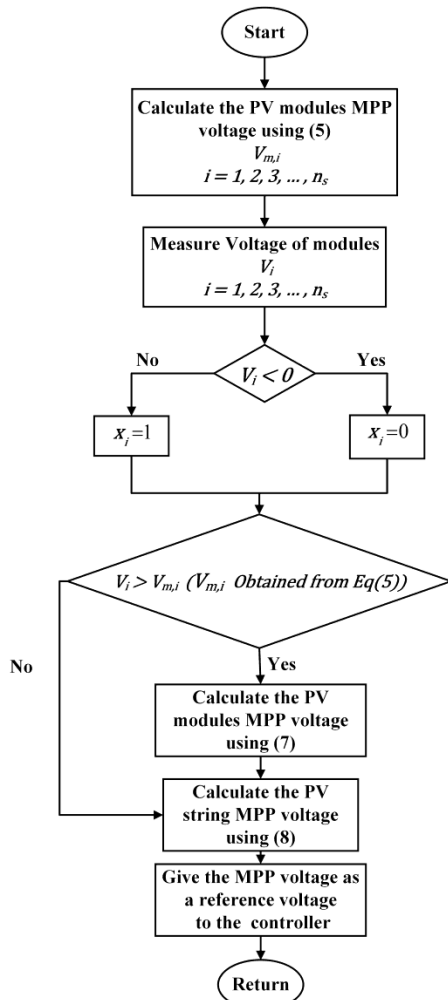

Fig. 7. The flowchart of the proposed GMPP tracking method

Fig. 8 shows the schematic diagram of the overall PV system consisting of the PV string, the temperature and irradiation estimator block, the proposed GMPP tracking block, DC-DC boost converter, and its input voltage controller. As can be seen from this figure, the global maximum power point tracking block requires the information of the temperature and irradiation level of the PV modules within the PV string. Hence, in the sequel, the estimation method of PV modules' temperature and irradiation levels is presented.

5. THE ESTIMATION OF PV MODULES TEMPERATURE AND IRRADIATION LEVEL

To calculate the maximum power point voltage of PV

modules using Eq. (5), the temperature and irradiation levels of PV modules are required. These quantities can be measured via pyranometers and thermometers. However, using temperature and radiation sensors will increase the overall cost of the MPPT controller and decrease its reliability during sensor malfunction.
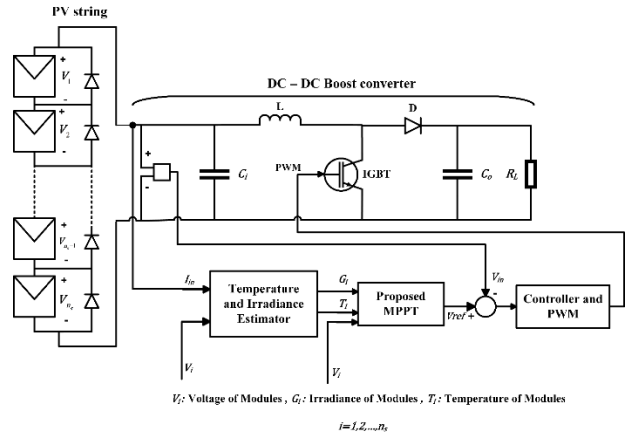

Fig. 8. The schematic diagram of the overall PV system consisting of A PV string, the temperature and irradiation estimator block, the GMPP tracking block, the DC-DC boost converter, and its input voltage controller

Therefore, to reduce costs and increase the system reliability, the temperature and irradiation levels of PV modules are estimated. To estimate these quantities, a current sensor to measure PV string output current and n_s voltage sensors to measure PV modules voltages are required where n_s is the number of PV modules within PV string. The approach by which the values captured by the voltage sensors are transferred to the converter depends on the distance between the PV string and the converter. In the low distances, the output of the voltage sensors as the voltage signals can be directly transmitted via a wiring connection between sensors and converter control system. However, in the long distances, the voltage signal transmission, may offer several problems. The series resistance between the sensors and the converter is a function of distance, the type of wire, temperature, etc. In these conditions, the voltage drops in the wiring system may cause significant errors in the estimation of the PV string GMPP voltage as well as inaccurate performance of the proposed GMPPT algorithm. In this situation, a possible solution is to use the current signal instead of voltage signal as a data carrying signal. The reason is that the current is constant in a loop irrespective of the proposed parameters such as distance, type of wires, temperature, etc. To do this, it is necessary to convert the voltage signal generated by the voltage sensors to electric current signal and then to transmit it. In the destination, besides of the converter, a reverse process is done, and the current signal is

converted to the voltage signal by passing through a resistor.

5.1. PV modules radiation estimation

To estimate radiation, according to the method presented in Ref. [17], first the photocurrents of PV modules within PV string are estimated by Eq. (10). Next, the PV module radiation is calculated via Eq. (11).

$$I_{ph,i} = I + I_0 \left[exp\left(\frac{V_i + IR_s}{aV_t}\right) - 1 \right] + \frac{V_i + IR_s}{R_p} \qquad (10)$$

$$G_i = \frac{I_{ph,i}G_n}{I_{ph,n}} \qquad (11)$$

where $i=1,2,...,n_s$. In these relations the value of I is measured only by a current sensor, and the PV modules' voltages are measured using voltage sensors whose numbers are equal to the number of PV modules within the PV string. It is noted although the values of R_p, R_s and a change with the variation of the PV module temperature and irradiation level [30], however, since their effect is minimal on the value of I_{ph}, all these parameters are calculated at STC conditions. Furthermore, it should be noted that the estimated values for PV modules' temperature and irradiation levels are not correct when the modules are shorted by their bypass diodes. This is because in these conditions, the voltage across shorted PV modules is approximately zero. However, it does not matter because when PV modules are short-circuited, they do not contribute in the PV power generation and there is no need for their radiation information. The effect of these modules is considered as the negative of the bypass diode forward biased voltage in Eq. (9).

5.2. PV modules temperature estimation

After estimating of PV modules' radiation levels (G_i), their surface temperatures are estimated by Eq. (12) [35].

$$GA_m = VI + U_{pv}A_m\left(T - T_a\right) \qquad (12)$$

where U_{pv} is the overall heat exchange coefficient, A_m is the area of the PV module surface, and T_a is the ambient temperature. Similar to the case of the irradiation estimation, the estimated value of the PV temperature will be invalid when PV modules are short-circuited by their antiparallel bypass diodes. Therefore, the amounts of temperature and irradiation levels are estimated correctly just when PV modules generate power. This is not a matter because according to the proposed method, the values of the temperature and irradiation levels are required only in the case that the PV modules contribute to the PV power generation.

6. RESULTS AND DISCUSSION

This section deals with the simulation results of the proposed GMPP tracking technique and compares it with three other model-based GMPP tracking methods. It is noted that using computer simulations is an effective way to compare different MPPT methods, since any temperature and irradiation pattern can be considered by it with a high level of flexibility [34]. In this paper, all the simulations are performed in MATLAB/Simulink. The PV module used in the PV string is MSX60, and its specifications are given in Table 1. A DC-DC boost converter is used to regulate PV string output voltage at the GMPP voltage, and its designed parameters are given in Table 2.

Table 1.   Catalogue values of the PV module MSX60

Module Parameters at STC	Values
Maximum Power (P_{max})	60 W
Open Circuit Voltage ($V_{oc,n}$)	21.1 V
Maximum Power Voltage (V_m)	17.1 V
Short Circuit Current ($I_{sc,n}$)	3.8 A
Maximum Power Current (I_m)	3.5 A
Number of Series Cells (N_s)	36
Temperature Coefficient of I_{sc} (k_i)	3 $\frac{mA}{°C}$
Temperature Coefficient of V_{oc} (k_v)	-0.08 $\frac{V}{°C}$
Overall heat exchange (U_{pv})	28.8 $\frac{W}{m^2 \, °K}$
PV module area (A_m)	0.5547 m^2

Table 2.   The designed parameters for the DC-DC boost converter

Parameters	Values
Input Capacitor (C_i)	20 μF
Inductor (L)	12 mH
Inductor Resistance (r_L)	0.01 Ω
ON State Resistance of the Switch (R_{on})	0.1 Ω
Diode Forward Voltage Drop (V_d)	0.8 V
Switching Frequency (f_s)	20 kHz
Output Capacitor (C_o)	15 μF
Load Resistance (R_L)	170 Ω

The three methods presented [21, 22, 25] are compared with the proposed technique under 10 different irradiation patterns given in Table 3, in a PV string consisting of 10 modules, see Fig. 5. The comparison between these methods is done from the viewpoint of the GMPP estimation accuracy. The results

of the comparison between the proposed technique and the methods presented in references [21, 22, 25] are given in Table 4. In this table, $V_{est,mpp}$ is the estimated GMPP voltage, and E_{ev} is the error percentage in the GMPP voltage estimation given by Eq. (13).

$$E_{ev} = \frac{\left|V_{est,mpp} - V_{act,mpp}\right|}{V_{act,mpp}} \times 100 \qquad (13)$$

where $V_{act,mpp}$ is the actual value of GMPP voltage. Moreover, E_{pt} is the error percentage in the estimation of GMPP power, and its value is given by Eq. (14).

$$E_{pt} = \frac{\left|P_{est,mpp} - P_{act,mpp}\right|}{P_{act,mpp}} \times 100 \qquad (14)$$

In Eq. (14), $P_{est,mpp}$ and $P_{act,mpp}$ are the estimated and actual values of the GMPP power, respectively.

In Table 4, for the 7th, 9th and 10th irradiation patterns of Table 3, the method in Ref. [29] was not able to give an accurate estimation of the GMPP. Furthermore, the proposed method in Ref. [21] gives the GMPP with a high error value for the 4th irradiation pattern of Table 3. The method in Ref. [22] does not give a correct value of the GMPP corresponding to the 7th irradiation pattern of Table 3. The maximum errors on the estimation of the GMPP voltage and power by the suggested method are 3.67% and 2.36% respectively. The average error value in the estimation of the global maximum power by the proposed technique and the methods in references [21, 22, 25] for the 10 radiation patterns of Table 3 are 0.5850%, 3.8057%, 7.1015% and 2.0889% respectively. These results prove that the statistical performance of the proposed GMPP tracking method is superior than that of the existing works in references [21, 22, 25]. It is noted that Ref. [21] and Ref. [22], have not used any estimation method for the evaluation of the temperature and irradiation levels of the PV modules. The estimation method proposed in Ref. [29] is exactly the same as the one employed in our work.

Table 3. 10 different irradiation patterns for the comparative studies between the proposed GMPP technique and the methods presented in references [21, 22, 27]

	Cases									Irradiance of modules $\left(\frac{W}{m^2}\right)$
1	G_1=1000	G_2=100	G_3=1000	G_4=700	G_5=700	G_6=700	G_7=200	G_8=200	G_9=200	G_{10}=1000
2	G_1=100	G_2=100	G_3=100	G_4=600	G_5=600	G_6=600	G_7=800	G_8=800	G_9=1000	G_{10}=1000
3	G_1=200	G_2=200	G_3=1000	G_4=1000	G_5=1000	G_6=1000	G_7=1000	G_8=1000	G_9=200	G_{10}=200
4	G_1=1000	G_2=800	G_3=700	G_4=700	G_5=700	G_6=200	G_7=200	G_8=200	G_9=200	G_{10}=200
5	G_1=800	G_2=800	G_3=700	G_4=600	G_5=600	G_6=500	G_7=500	G_8=300	G_9=300	G_{10}=100
6	G_1=1000	G_2=1000	G_3=1000	G_4=1000	G_5=1000	G_6=200	G_7=200	G_8=200	G_9=200	G_{10}=200
7	G_1=700	G_2=500	G_3=1000	G_4=500	G_5=1000	G_6=700	G_7=1000	G_8=500	G_9=700	G_{10}=1000
8	G_1=1000	G_2=300	G_3=900	G_4=800	G_5=800	G_6=800	G_7=300	G_8=300	G_9=300	G_{10}=900
9	G_1=1000	G_2=1000	G_3=1000	G_4=1000	G_5=1000	G_6=700	G_7=700	G_8=700	G_9=700	G_{10}=700
10	G_1=900	G_2=900	G_3=900	G_4=100	G_5=100	G_6=100	G_7=600	G_8=600	G_9=600	G_{10}=600

Table 4. The results of GMPP voltage and power estimations and their corresponding errors by the proposed technique and the methods in references [21, 22, 27]

Cases		1	2	3	4	5	6	7	8	9	10
Proposed method	$V_{est,mpp}$	96.81	111.10	87.19	74.48	112.30	71.33	163.70	88.60	160.70	114.30
	E_{ev} %	3.67	1.02	0.38	1.56	2.16	0.02	2.32	2.34	0.21	2.60
	P_{mpp}	227.80	240.10	306.2	187.30	203.30	250.50	297.30	259	402.10	233.90
	E_{pt} %	2.36	0.1	0.06	0.19	0.63	0.04	0.91	0.52	0.05	0.99
The method in [27]	$V_{est,mpp}$	96.53	112.41	90.93	81.34	114.84	79.18	55.84	96.18	76.78	191.31
	E_{ev} %	3.51	0.14	4.09	7.51	0.05	11.04	66.72	6.01	52.12	71.71
	P_{mpp}	228.50	240.30	301.8	173.20	204.5	222.70	194.80	249.10	238.60	65.81
	E_{pt} %	1.92	0.02	1.50	7.71	0.04	11.13	35.07	4.32	68.60	72.14
The method in [21]	$V_{est,mpp}$	101.94	119.20	83.57	87.02	117.99	76	173.88	98.08	169.91	120.07
	E_{ev} %	9.31	6.19	4.52	15.01	2.80	6.58	3.53	8.10	5.96	7.78
	P_{mpp}	192	219.50	303	120	200.20	242.10	288.80	236.70	376.70	209.10
	E_{pt} %	17.72	8.90	1.11	36.06	2.15	3.39	3.74	9.08	6.36	11.50
The method in [22]	$V_{est,mpp}$	84.25	110.80	81.20	73.25	112.82	71	127.25	87.48	159.5	98.4
	E_{ev} %	9.66	1.29	7.23	3.19	1.71	0.43	24.23	3.58	0.54	11.67
	P_{mpp}	219.60	239.90	298.40	186.10	203.70	250.40	242.40	257.50	402.20	218.20
	E_{pt} %	5.89	0.18	2.61	0.84	0.43	0.08	19.21	1.09	0.04	7.64
$V_{act,mpp}$ (V)		93.26	112.25	87.53	75.66	114.78	71.31	167.95	90.73	160.36	111.40

P_{act} (W)			233.34	240.35	306.39	187.67	204.59	250.60	300.02	260.35	402.28	236.25

Table 5.   Irradiation patterns used in time simulations of a PV string consisting 10 PV modules

Time (s)	Irradiance of modules $\left(\frac{W}{m^2}\right)$									
0 – 0.08	G_1=1000	G_2=900	G_3=800	G_4=700	G_5=600	G_6=500	G_7=400	G_8=300	G_9=200	G_{10}=100
0.08 – 0.16	G_1=900	G_2=900	G_3=900	G_4=600	G_5=600	G_6=600	G_7=600	G_8=100	G_9=100	G_{10}=100
0.16 – 0.24	G_1=1000	G_2=1000	G_3=1000	G_4=700	G_5=700	G_6=500	G_7=500	G_8=500	G_9=100	G_{10}=100
0.24 – 0.32	G_1=1000	G_2=700	G_3=500	G_4=900	G_5=600	G_6=1000	G_7=600	G_8=100	G_9=600	G_{10}=600

Table 6.   A more precise investigation of the proposed GMPP method's speed and accuracy

Time (s)	$V_{act,mpp}$(V)	$V_{est,mpp}$(V)	P_{act} (W)	P_{mpp}(W)	E_{ev} %	E_{pt}%	Tracking time (s)
0-0.08	98.65	96.22	178.1	175.89	2.46	1.24	0.012
0.08 - 0.16	111.3	110.2	236.2	235.77	0.99	0.18	0.006
0.16 - 0.24	131.95	129.2	234.3	232.51	2.08	0.76	0.005
0.24 - 0.32	151.62	152	275.3	275.1	0.25	0.07	0.004
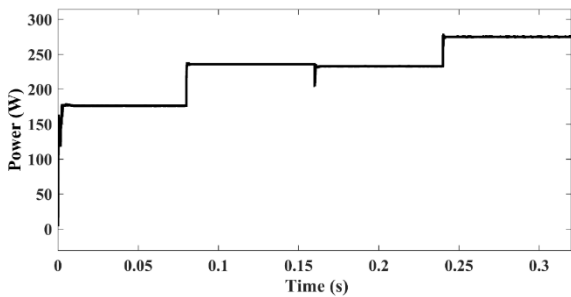
(a)
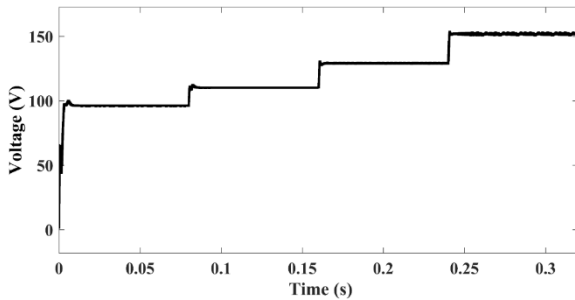
(b)

Fig. 9. The simulation results of the proposed GMPP tracking method for the radiation patterns of Table 5. (a) the output power, (b) the estimated GMPP voltage

In the sequel, the radiation pattern is changed in certain times to evaluate the dynamical performance of the proposed GMPP tracking method. These radiation patterns are given in Table 5. The PV string power and voltage profiles are shown in Fig. 9(a) and Fig. 9(b) respectively. Table 6 provides a more precise investigation from the GMPP tracking time and quality. According to this table, it is evident that the GMPP tracking time in the proposed method is very low during irradiation level changes.

Furthermore, as it can be seen from this table, the maximum error in tracking of the global maximum power is less than 2%. Fig. 10(a), Fig. 10(b), Fig. 10(c) and Fig. 10(d) illustrate the P-V curves of the PV string under different radiation patterns of Table 5. Moreover, the actual value of the global maximum power for each irradiation pattern is visible in these figures. The simulation results show that the performance of the proposed method is desirable from speed and accuracy point of views. An interesting nontrivial problem is to prove theoretically the convergence of the proposed algorithm to the GMPP. What is evident from the simulation results is that the proposed algorithm solves online a mixed integer nonlinear optimization problem to find its global optimum point.

The proposed algorithm finds the GMPP intelligently in the sense that it does not check all the local peak candidates given by Eq. (6) and Eq. (8). This can be observed, for example, from Figs. 9(b) and 10(a). While in Fig. 10(a), the range of local peak voltages belongs to the interval [0, 200] V, according to Fig. 9(b), the search span relies on the interval [0, 100] V. It should be noted that a limitation of the proposed model-based GMPPT technique is the voltage sensors connected to each PV module of the PV string to estimate PV modules radiation levels. At the first glance, this causes that in the practical implementation of the PV system, the overall cost increases due to the use of voltage sensors with the number of existing modules. However, since the cost of the radiation sensor (pyranometer) is much higher than that of the voltage sensor, the cost parameter

is improved by removing the radiation sensors. In general, the model-based methods are more costly than the heuristic-based algorithms. Nevertheless, the precision and especially the GMPP tracking speed in model-based methods is very high in a wide range of climatic conditions, which increases the efficiency of the overall system. These advantages compensate some parts of costs in the model-based tracking techniques. Furthermore, the information provided by the voltage sensors can be used to identify the type and location of any fault in the PV string [35].
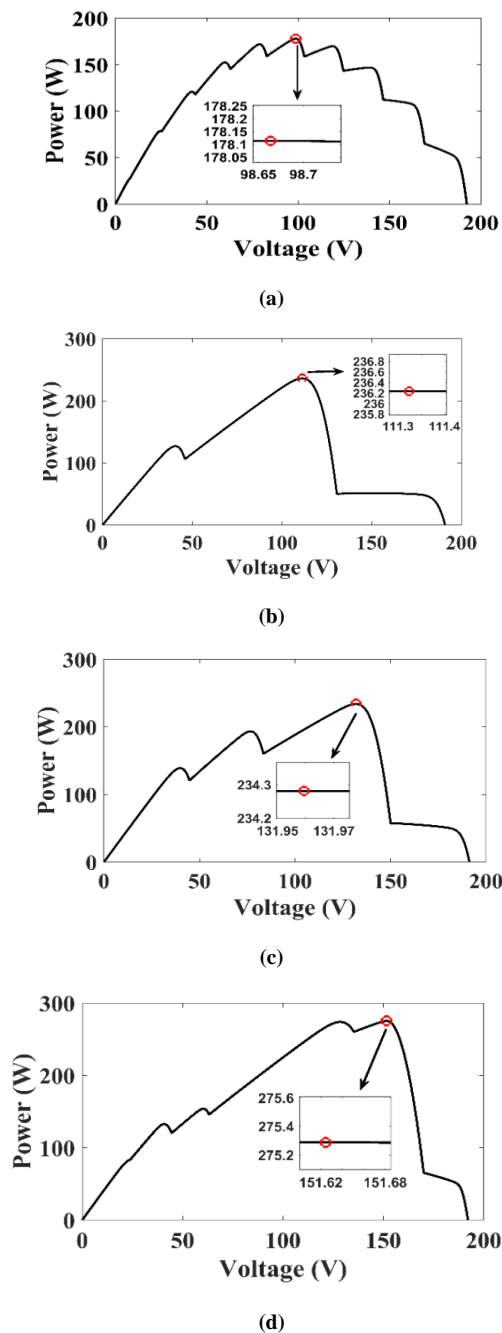

Fig. 10. P-V curves corresponding to the radiation patterns of Table 5. (a) P-V curve during time interval of (0-0.08) s, (b) P-V curve during time interval (0.08-0.16) s, (c) P-V curve during time interval (0.16-0.24) s, (d) P-V curve for the time interval (0.24-.32)

7. CONCLUSIONS

In this paper, a new model-based approach has been presented for the global maximum power point tracking of PV strings under partial shading conditions. The suggested GMPP tracking technique neither needs to solve numerically the implicit and nonlinear equations of the PV modules nor to use complex and time-consuming meta-heuristic algorithms. In contrast to the existing model-based techniques in which the coordinates of all local peaks of PV strings are estimated, in the proposed technique, the location of the GMPP is directly estimated without any need to evaluate the locations of other local peaks on the P-V curve. The simulation results show that the suggested method is accurate enough and its maximum errors on the estimation of the GMPP voltage and power are below 4% and 3% respectively. In addition, its GMPP tracking speed is below 15 ms, which is quite fast as compared with the time constants of irradiation changes in practice. The proposed technique was compared with three other model-based GMPP tracking methods, and the results confirmed its superior statistical performance as compared with the existing methods.

REFERENCES

[1] F. Belhachat and C. Larbes, "A review of global maximum power point tracking techniques of photovoltaic system under partial shading conditions," *Renew. Sust. Energy. Rev.,* vol. 92, pp. 513-553, 2018.

[2] A. Datta, G. Bhattacharya, D. Mukherjee, and H. Saha, "An efficient technique for controlling power flow in a single stage grid-connected photovoltaic system," *Sci. Iran. Trans. D,* vol. 21, no. 3, pp. 885, 2014.

[3] M. A. G. De Brito, L. Galotto, L. P. Sampaio, G. d. A. e Melo, and C. A. Canesin, "Evaluation of the main MPPT techniques for photovoltaic applications," *IEEE T. Ind. Electron.* vol. 60, no. 3, pp. 1156-1167, 2013.

[4] M. A. Mohamed, A. A. Z. Diab, and H. Rezk, "Partial shading mitigation of PV systems via different meta-heuristic techniques," *Renew. Energy,* 2018.

[5] A. Mohapatra, B. Nayak, P. Das, and K. B. Mohanty, "A review on MPPT techniques of PV system under partial shading condition," *Renew. Sust. Energy. Rev.,* vol. 80, pp. 854-867, 2017.

[6] J. Javidan, "Energy management strategy of stand-alone photovoltaic system in cathodic protection pipeline," *J. Oper. Autom. Power Eng*, vol. 4, pp. 143-152, 2016.

[7] A. Akhavan and H. Mohammadi, "A new control method for grid-connected quasi-Z-source multilevel inverter based photovoltaic system," *Sci. Iran. Trans. D,* vol. 6, no. 22, pp. 2505-2515, 2015.

[8] M. A. Ramli, S. Twaha, K. Ishaque, and Y. A. Al-Turki, "A review on maximum power point tracking for photovoltaic systems with and without shading conditions," *Renew. Sust. Energy Rev.,* vol. 67, pp. 144-159, 2017.

[9] T. Esram and P. L. Chapman, "Comparison of photovoltaic array maximum power point tracking

techniques," *IEEE T. Energy Conver.,* vol. 22, no. 2, pp. 439-449, 2007.

[10] A. Gupta, Y. K. Chauhan, and R. K. Pachauri, "A comparative investigation of maximum power point tracking methods for solar PV system," *Sol. Energy,* vol. 136, pp. 236-253, 2016.

[11] A.-M. I. Aldaoudeyeh, "Photovoltaic-battery scheme to enhance PV array characteristics in partial shading conditio conditions," *IET Renew. Power Gen.,* vol. 10, no. 1, pp. 108-115, 2016.

[12] M. Dhimish, V. Holmes, B. Mehrdadi, M. Dales, B. Chong, and L. Zhang, "Seven indicators variations for multiple PV array configurations under partial shading and faulty PV conditions," *Renew. Energy,* vol. 113, pp. 438-460, 2017.

[13] H. Labar and M. S. Kelaiaia, "Real time partial shading detection and global maximum power point tracking applied to outdoor PV panel boost converter," *Energy Convers. Manage,* vol. 171, pp. 1246-1254, 2018.

[14] M. A. Ghasemi, H. M. Forushani, and M. Parniani, "Partial shading detection and smooth maximum power point tracking of PV arrays under PSC," *IEEE T. Power Electr.,* vol. 31, no. 9, pp. 6281-6292, 2016.

[15] M. S. El-Dein, M. Kazerani, and M. Salama, "Optimal photovoltaic array reconfiguration to reduce partial shading losses," *IEEE T. Sustain. Energy,* vol. 4, no. 1, pp. 145-153, 2013.

[16] B. I. Rani, G. S. Ilango, and C. Nagamani, "Enhanced power generation from PV array under partial shading conditions by Shade dispersion using Su Do Ku configuration," *IEEE T. Sustain. Energy,* vol. 4, no. 3, pp. 594-601, 2013.

[17] G. Velasco-Quesada, F. Guinjoan-Gispert, R. Piqué-López, M. Román-Lumbreras, and A. Conesa-Roca, "Electrical PV array reconfiguration strategy for energy extraction improvement in grid-connected PV systems," *IEEE T. Ind. Electron.,* vol. 56, pp. 4319-4331, 2009.

[18] K. Ishaque and Z. Salam, "A deterministic particle swarm optimization maximum power point tracker for photovoltaic system under partial shading condition," *IEEE T. Ind. Electron.,* vol. 60, pp. 3195-3206, 2013.

[19] S. Mohanty, B. Subudh and P. Ray, "A grey wolf-assisted perturb & observe MPPT algorithm for a PV system," *IEEE T. Energy Conver.,* vol. 32, pp. 340-347, 2016.

[20] R. Aghaie, M. Farshad, "Maximum power point tracker for photovoltaic systems based on moth-flame optimization considering partial shading conditions," *J. Oper. Autom. Power Eng.,* vol. 7, pp. 176-186, 2019.

[21] J. Ahmed and Z. Salam, "An improved method to predict the position of maximum power point during partial shading for PV arrays," *IEEE T. Ind. Inform.,* vol. 11, no. 6, pp. 1378-1387, 2015.

[22] E. I. Batzelis, I. A. Routsolias, and S. A. Papathanassiou, "An explicit PV string model based on the lambert $ W $ function and simplified MPP expressions for operation under partial shading," *IEEE T. Sustain. Energy,* vol. 5, no. 1, pp. 301-312, 2014.

[23] G. N. Psarros, E. I. Batzelis and S. A. Papathanassiou, "Partial shading analysis of multistring PV arrays and derivation of simplified MPP expressions," in *IEEE T. Sustain. Energy,* vol. 6, no. 2, pp. 499-508, 2015.

[24] S. M. Hashemzadeh, "A new model-based technique for fast and accurate tracking of global maximum power point in photovoltaic arrays under partial shading conditions", *Renewable Energy,* vol. 139, pp. 1061-1076, 2019.

[25] L. Cristaldi, M. Faifer, M. Rossi, and S. Toscani, "An improved model-based maximum power point tracker for photovoltaic panels," *IEEE T. Instrum. Meas.,* vol. 63, no. 1, pp. 63-71, 2014.

[26] Y. Mahmoud, M. Abdelwahed, and E. F. El-Saadany, "An enhanced MPPT method combining model-based and heuristic techniques," *IEEE T. Sustain. Energy,* vol. 7, no. 2, pp. 576-585, 2016.

[27] Y. Mahmoud and E. F. El-Saadany, "Fast power-peaks estimator for partially shaded PV systems," *IEEE T. Energy Conver.,* vol. 31, no. 1, pp. 206-217, 2016.

[28] E. V. Paraskevadaki and S. A. Papathanassiou, "Evaluation of MPP voltage and power of mc-Si PV modules in partial shading conditions," *IEEE T. Energy Conver.,* vol. 26, no. 3, pp. 923-932, 2011.

[29] M. G. Villalva, J. R. Gazoli, and E. Ruppert Filho, "Comprehensive approach to modeling and simulation of photovoltaic arrays," *IEEE T. Power Electr.,* vol. 24, no. 5, pp. 1198-1208, 2009.

[30] M. Hejri, H. Mokhtari, M. Azizian, M. Ghandhari, and L. Soder, "On the parameter extraction of a five-parameter double-diode model of photovoltaic cells and modules," *IEEE J. Photovoltaic,* vol. 4, pp. 915-923, 2014.

[31] M. Hejri, H. Mokhtari, M. R. Azizian, and L. Söder, "An analytical-numerical approach for parameter determinati-on of a five-parameter single-diode model of photovoltaic cells and modules," *Int. J. Sustainable Energy,* vol. 35, no. 4, pp. 396-410, 2016.

[32] M. Hejri and H. Mokhtari, "On the comprehensive parametrization of the photovoltaic cells and modules," *IEEE J. Photovoltaic,* vol. 7, pp. 250-258, 2017.

[33] Y. Hu, W. Cao, J. Ma, S. J. Finney, and D. Li, "Identifying PV module mismatch faults by a thermography-based temperature distribution analysis," *IEEE T. Device Mat. Re.,* vol. 14, pp. 951-960, 2014.

[34] M. Uoya and H. Koizumi, "A calculation method of photovoltaic array's operating point for MPPT evaluation based on one-dimensional Newton–Raphson method," *IEEE T. Ind. Appl.,* vol. 51, no. 1, pp. 567-575, 2015.

[35] S. Moballegh and J. Jiang, "Modeling, prediction, and experimental validations of power peaks of PV arrays under partial shading conditions," *IEEE T. Sustain. Energy,* vol. 5, no. 1, pp. 293-300, 2014.